Styrene/Tetradecyl Methyl Acrylate/3-Methacryloxylpropyl Trimethoxyl Silane Triblock Copolymers: Atom Transfer Radical Polymerization Synthesis and Effects on the Glass-Fiber/Polypropylene Interphase Properties as a Macromolecular Coupling Agent

Shanhua Zhou,[1] Yan Gao,[1,2] Yantao Wang,[1,2] Chunpu Hu,[1,2] Qingzhi Dong[1,2]

[1]*School of Materials Science and Engineering, East China University of Science and Technology, Shanghai 200237, People's Republic of China*
[2]*Key Laboratory for Ultrafine Materials, Ministry of Education, Shanghai 200237, People's Republic of China*

Received 26 April 2006; accepted 14 November 2006
DOI 10.1002/app.25793
Published online in Wiley InterScience (www.interscience.wiley.com).

ABSTRACT: Styrene/tetradecyl methyl acrylate/3-methacryloxylpropyl trimethoxyl silane triblock copolymers (PSTKs), with well-defined structures and narrow molecular weight distributions, were synthesized by atom transfer radical polymerization. They were investigated as macromolecular coupling agents for the surface treatment of glass fibers. The reaction kinetics for the triblock copolymers were studied. The contact angles of the copolymers with water and diiodomethane showed that a modified-glass-fiber surface treated with a PSTK solution had strong hydrophobicity and that the impregnation of polypropylene on glass fibers was improved dramatically. In comparison with a film of 3-methacryloxylpropyl trimethoxyl silane, the polarity of the surface free energy of a PSTK film decreased, whereas the dispersion increased greatly. The critical concentration of the macromolecular coupling agents was obtained, and the monolayer saturated adsorptive capacity was calculated with the Gibbs absorption isotherm equation. © 2007 Wiley Periodicals, Inc. J Appl Polym Sci 104: 1661-1670, 2007

Key words: atom transfer radical polymerization (ATRP); block copolymers; composites; fibers; kinetics (polym.); polysiloxanes

INTRODUCTION

The hydrophilic character of glass fibers leads to low compatibility and wetting with a hydrophobic polypropylene matrix and therefore poor adhesion between the glass fibers and the matrix. However, the final performance of composites depends largely on that kind of adhesion. To improve the wetting and adhesion between glass fibers and a polypropylene matrix, the introduction of modifiers such as maleic anhydride grafted polypropylene onto the surface of glass fibers, mostly treated with organosilane coupling agents, has been reported.[1-6] Recent developments on macromolecular coupling agents with special structures have been emphasized because the efficiency is superior to that of organosilane coupling agents and profits from the long molecular chains of the hydrophobic components.[7,8]

The preparation methods for copolymers used as macromolecular coupling agents include random copolymerization, living anionic copolymerization, and atom transfer radical polymerization (ATRP).[9-18] Among them, ATRP is a good living polymerization method for obtaining copolymers coated onto glass fibers.[16-18] Moreover, copolymers can be directly attached onto the surface of glass by surface-initiated ATRP with the chlorinated silica surface of glass as an effective macroinitiator.[19-23]

In this study, styrene/tetradecyl methyl acrylate/3-methacryloxylpropyl trimethoxyl silane triblock copolymers (PSTKs), used as macromolecular coupling agents for glass fiber/polypropylene, were synthesized by ATRP under moderate conditions. These triblock copolymers had well-defined structures of predetermined molecular weights and narrow molecular weight distributions. When PSTKs were coated onto glass-fiber surfaces, the copolymers were readily subjected to hydrolysis and grafted onto the glass-fiber surfaces to generate self-assembled films. According to the impregnation theory of composite interfaces, the wetting of the matrix on glass fibers, which can be characterized by the contact angle and surface free energy, is critical for good interfacial adhesion. There-

Correspondence to: Q. Dong (qzdong@online.sh.cn).
Contract grant sponsor: China Petroleum & Chemical Corp.; contract grant number: X505010.

Journal of Applied Polymer Science, Vol. 104, 1661-1670 (2007)
© 2007 Wiley Periodicals, Inc.

fore, the effect of the macromolecular coupling agent PSTK on the contact angle and surface free energy of glass fibers was investigated. The wetting of polypropylene on glass fibers could be greatly improved by PSTK coated onto the glass fibers because the hydrophilic group Si—O—CH_3 of PSTK could react with —OH of the glass fibers and the hydrophobic components [tetradecyl methacrylate (TMA) and styrene (St)] of PSTK had good wetting and compatibility with polypropylene. When the surface free energy of glass fibers did not decrease with increasing concentration, the critical concentration of the triblock copolymer PSTK solution was reached, and this meant that the wetting and adhesion of polypropylene on the glass fibers would no longer be improved. At this point, the adsorption was in a monolayer saturated state, and the optimum concentration often could be found near this concentration. The area of a single macromolecule was calculated according to the monolayer adsorptive capacity. The ratio of poly(tetradecyl methacrylate) (PTMA) blocks to polystyrene (PS) blocks in PSTK was estimated with this area and was consistent with the energy spectrum results.

EXPERIMENTAL

Materials

St (Shanghai Chemical Reagent Co., Shanghai, China; chemically pure) was stirred in the presence of CaH_2 for 24 h and was distilled before use. TMA (Shanghai Refinery, Shanghai, China; chemically pure) was purified by the removal of the polymerization inhibitor with a sodium hydroxide solution, washed to neutrality with water (H_2O), stirred over calcium hydride overnight, and distilled before use. 3-Methacryloxylpropyl trimethoxyl silane (KH570; Shanghai Sipu Chemical Reagent Co., Shanghai, China; analytical reagent) was used as received. Toluene (Shanghai Chemical Reagent; analytical reagent) was refluxed for 24 h in the presence of sodium wire. All monomers and toluene were deoxygenated and purged with nitrogen before use. CuBr (Shanghai Chemical Reagent; analytical reagent) was purified as described in the literature.[24] 2,2′-Bipyridine (bpy; Shanghai Chemical Reagent No. 1 Plant, Shanghai, China; analytical reagent) was recrystallized from hexane three times. Pentamethyldiethylenetriamine (PMDETA) and ethyl α-bromoisobutyrate (EBriB; Lancaster; >98%) were purchased from Aldrich (Shanghai, China) and used as received. Polypropylene was offered by Shanghai Jinshan Petroleum Co. (Shanghai, China). N_2 (Shanghai Wugang Gas Co., Ltd., Shanghai, China; 99.9%) was used as received.

Polymerization

In a typical monofunctional poly(styrene) (PSt-Br) polymerization via ATRP [sample PSt-Br-3 in Table V (shown later)], CuBr (9.6×10^{-4} mol) was added to a dry 20-mL, flat-bottom flask equipped with a stirring bar. After being sealed with a rubber tube, the flask was degassed and backfilled with nitrogen three times and then was left under nitrogen. At the same time, the system was stirred for 30 min. PMDETA (1.92×10^{-3} mol) and 4 mL of toluene were added, and the solution was stirred it was clarified. St (3.50×10^{-2} mol) was added successively. After the mixture became homogeneous, EBriB (9.6×10^{-4} mol) was added to the flask via a syringe that had been purged with nitrogen. Then, the flask was placed in a 65°C oil bath for 21.5 h. The flask was cooled and diluted by toluene after the reaction was finished, and then the mixture was precipitated with excess methanol. The yield was determined by gravimetry. The weight of the catalyst was subtracted from the total mass of the product to obtain the weight of the polymer product. The mixture was purified by dissolution in toluene and passed through a neutral alumina column to remove the catalyst. The polymer was precipitated with excess methanol, collected by filtration, and then dried *in vacuo* at 30°C for 24 h. The synthesis of the PSTK triblock copolymer was like the synthesis of the macroinitiator. The difference was that when PSTK was synthesized (sample 2#PSTK), PSt-Br (2.31×10^{-3} mol) was used as the initiator instead of EBriB. The reaction needed more time. In addition, when the conversion of TMA (1.135×10^{-2} mol) almost approached 100%, the solution was cooled to room temperature, then KH570 (1.65×10^{-2} mol) was added, and the solution was stirred for the preset time at 90°C. The synthetic routes of the macroinitiator and triblock copolymer are shown in Figure 1.

Polymer characterization

The molecular weights and molecular weight distributions of the macroinitiators and triblock copolymers were determined with ^{1}H-NMR and a Waters 150C gel permeation chromatography (GPC) apparatus. The apparatus consisted of a Waters 510 high-performance liquid chromatography pump and a Waters 410 differential refractometer, and tetrahydrofuran was used as the solvent for PSt-Br and PSTK, with calibrations based on standard PS. ^{1}H-NMR was carried out on a Bruker 500 spectrometer with $CDCl_3$ as the solvent. Fourier transform infrared (FTIR) spectra of the macroinitiators and triblock copolymers were recorded on a Nicolet Magna IR550 spectrometer. The C/Si/O weight ratio was determined by energy spectroscopy, and the St/TMA/KH570 weight ratio of the copolymers was then calculated.

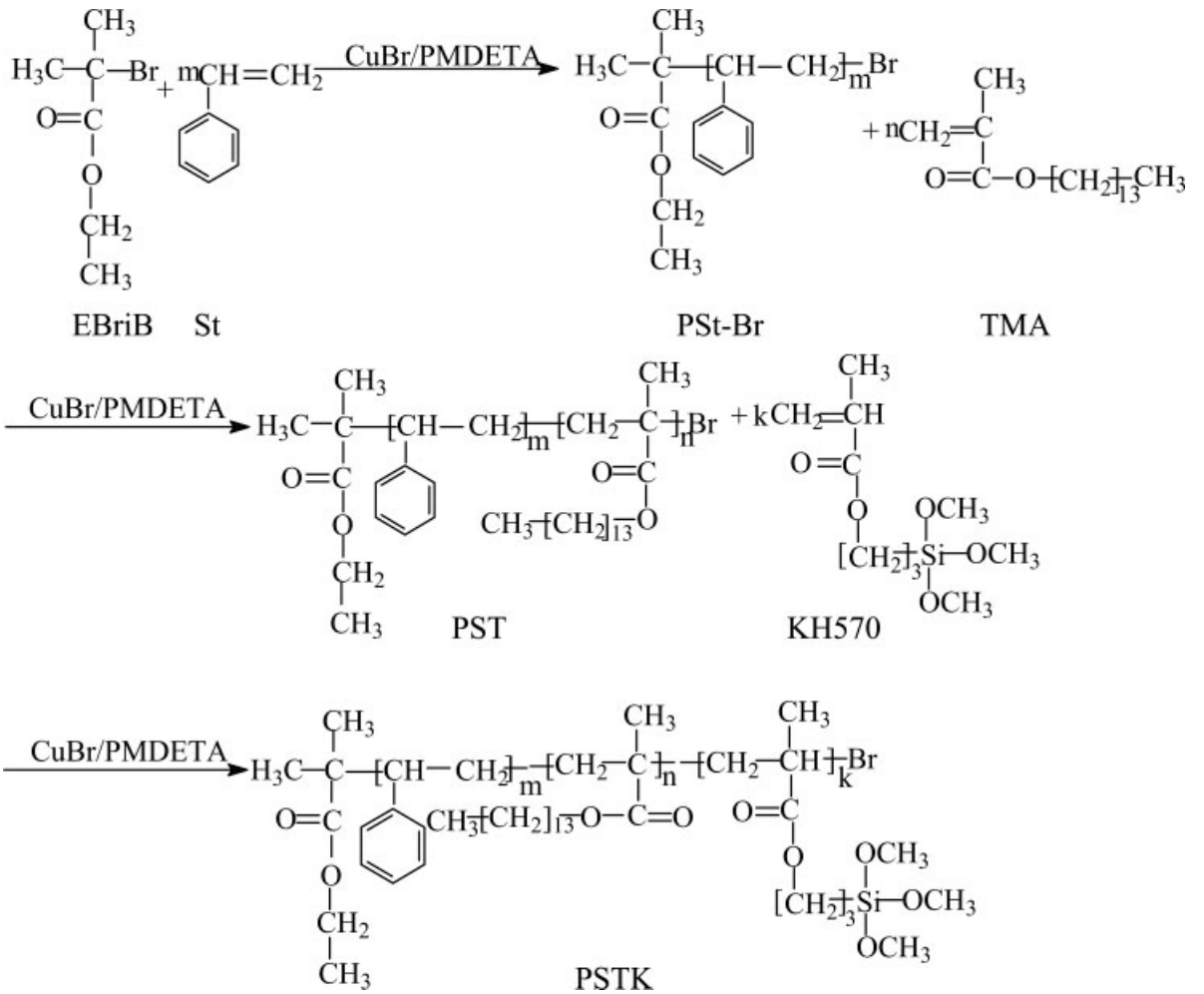

Figure 1 Synthetic route of the triblock copolymer.

Contact-angle measurements

For a glass fiber 17 μm in diameter, the direct measurement of the contact angle was difficult and involved complicated numerical analysis of the expressions for the liquid drop profile on the fibers.[25,26] Therefore, the contact angles were directly measured from a 4-mL drop of liquid placed on a triblock copolymer coated on a glass plate by spin coating with a microsyringe. Distilled H_2O and diiodomethane (CH_2I_2) were employed, with three measurements for each liquid.

RESULTS AND DISCUSSION

Synthesis of the PSt-Br macroinitiator

Block sequence

The rate constants of activation (k_{act}) and deactivation (k_{dact}) are both defined as pseudo-first-order constants. Because the fracture energy of C—Br in initiator EBriB was smaller than that of C—Br in PSt-Br and PTMA-Br, which made the rate constant of activation of initiation greater than the that of propagation, all the initiator (EBriB) was converted into macroinitiator (RM_iBr) in the first stage of polymerization, and the initiation efficiency was almost 100%.

One of the important factors was the quick dynamic equilibrium between the active and dormant species, which controlled the number of propagating radicals, and the reaction rate was controlled by the chain propagation rate. Table I indicates that the conversion of TMA could reach 90.6% in 0.7 h, whereas the conversion of St was only 66.7% in 6.0 h under the same conditions; this proved that the propagation rate of TMA was significantly higher than that of St, and the apparent rate constant (k_p^{app}) of TMA was greater than that of St.

Scheme 1 shows the polymerization mechanism when the macroinitiator is used.

Table II shows that the conversion of St with macroinitiator PTMA-Br was smaller than the conversion of TMA with macroinitiator PSt-Br under the same conditions, and this confirmed that the initiation efficiency of PSt-Br was higher than that of PTMA-Br, although k_p^{app} of TMA was greater

TABLE I
Homopolymerization Reaction Velocities of the Different Monomers[a]

Monomer	Feed ratio ($\times 10^4$ mol)[b]	Time (h)	Yield (%)	$M_{n,GPC}$	$M_{n,theo}$[c]	M_w/M_n
TMA	189.4/8.3	0.7	90.6	6820	6000	1.12
St	524.4/6.3	6.0	66.7	6210	6000	1.18

[a] Reaction temperature = 70°C; bulk polymerization; [EBriB]/[CuBr]/[PMDETA] = 1 : 1 : 2.
[b] [Monomer]/[EBriB].
[c] $M_{n,theo}$ = Yield (%) × [Monomer]/[Initiator] × M_n(monomer) + M_n(initiator).

than that of St. Because the C—Br fracture energy of the macroinitiator in initiation was higher than that of macroinitator ($RM_n^aM_i^bX$) in propagation with macroinitiator PTMA-Br, the rate constant of activation in the initiation reaction ($k_{act,1}$) was lower than that in the propagation reaction ($k_{act,2}$): $k_{act,1} \ll k_{act,2}$. Therefore, the initiation efficiency of PTMA-Br was low (Scheme 1), and this led to a low yield of St. Accordingly, the macroinitiator PSt-Br instead of PTMA-Br should be synthesized, and then TMA and KH570 were added in sequence to prepare the triblock copolymer PSTK with a preset molecular weight.

Reaction kinetics of the PSt-Br macroinitiator

Figure 2 shows the kinetic curves for the ATRP of St at different temperatures. The monomer conversion increased with the reaction time, and the kinetic plot of $\ln([M]_0/[M])$ versus time (where [M] is the monomer concentration and $[M]_0$ is the initial monomer concentration) was linear with linear regression coefficients of 0.9918 and 0.9919, respectively, which supported the living character of ATRP. In addition, the dependence of the GPC-determined number-average molecular weight ($M_{n,GPC}$) and the weight-average molecular weight/number-average molecular weight (M_w/M_n) ratio on the conversion in the polymerization of St at 65°C is shown by Figure 3. $M_{n,GPC}$ increased linearly with an increasing yield.

k_p^{app} at different temperatures was calculated by the slope of the curve, and the concentration of the active species ([P·]) could be obtained with the following equations:

$$R_p = -d[M]/dt = k_p[P\cdot][M] = k_p^{app}[M] \quad (1)$$

$$\ln([M_0]/[M]) = k_p^{app}t \quad (2)$$

$$[P\cdot] = k_p^{app}/k_p \quad (3)$$

where R_p is the propagation rate, k_p is the propagation rate constant, and t is the reaction time.

The kinetic data for the solution polymerization of St are listed in Table III. The concentrations of the dormant species, which equaled the difference value between the concentration of the initiator (0.151 mol/L) and [P·] (1.90×10^{-7} mol/L, 2.48×10^{-7} mol/L), were far higher than [P·] at 65 and 75°C. Therefore, [P·] was always low in the reaction, and this resulted in a narrow molecular weight distribution, which also agreed with the living character of ATRP.

According to eq. (4), the apparent activation energy (E_p^{app}) and frequency factor (A_p^{app}) of the polymerization could be obtained by k_p^{app} at different temperatures. A_p^{app} of St via solution ATRP was low and compared well with that in the literature;[28] this indicated that there was only a minor effect of temperature on the ATRP reaction rate of St:

$$\ln(k_p^{app,St}) = \ln A_p^{app,St} - E_p^{app,St}/R \times T \quad (4)$$

where T is the temperature and R is the gas constant in the ideal gas equation.

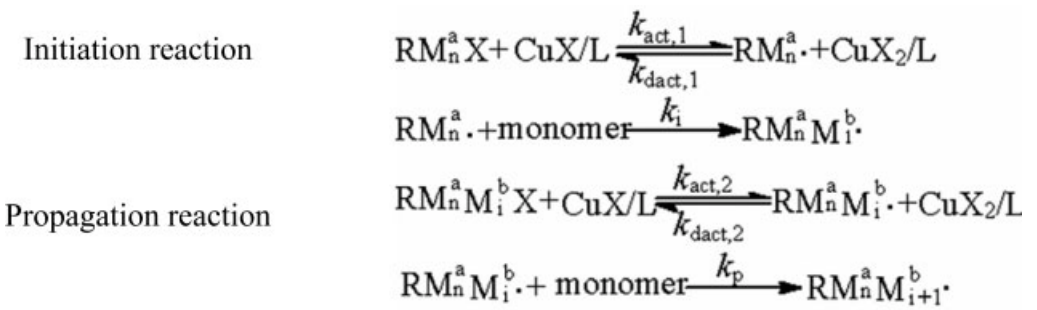

Scheme 1 Mechanism of initiation and propagation.

TABLE II
Effect of the Initiation Sequence on the Yield[a]

Monomer	Initiator	Feed ratio ($\times 10^4$ mol)[b]	Yield (%)	$M_{n,GPC}$	$M_{n,theo}$[c]	M_w/M_n
St	PTMA-Br	524.4/3.3	36.0	17,820	12,000	1.12
TMA	PSt-Br	189.4/8.0	89.5	18,110	12,000	1.34

[a] Temperature = 90°C; solvent = toluene; reaction time = 30 h; [EBriB]/[CuBr]/[PMDETA] = 1 : 5 : 10.
[b] [Monomer]/[Initiator].
[c] $M_{n,theo}$ = Yield (%) × [Monomer]/[Initiator] × M_n(monomer) + M_n(initiator).

Effect of the ligand on the yield of the PSt-Br macroinitiator

Ligands and solvents can significantly change electronic, steric, and solubility properties of copper catalysts, thus tuning the kinetic behaviors of the system. According to Table IV, the yield was 82% at 100°C with bpy as the ligand of CuBr, whereas the yield could reach 81% at 85°C with PMDETA; this indicated that a similar conversion of the PS homopolymer could be obtained with PMDETA as the ligand at a lower temperature and concentration than with bpy. It can be illustrated that copper complexes with PMDETA possess lower redox potentials than those with bpy, and this leads to a higher k_{act} value and a lower k_{dact} value and then a higher reaction rate.[29]

Effect of the reaction time and temperature on the yield of the PSt-Br macroinitiator

The yield increased rapidly with the reaction time at 65°C, but the yield increased slightly when the reaction time exceeded 21.5 h, as illustrated in Table V, so the reaction time of 21.5 h was chosen. With the temperature increased by 10°C, the yield of PSt-Br-4 was 15.6% higher than that of PSt-Br-2, and this indicated that the temperature had a great effect on the yield.

Kinetic study of the solution polymerization of TMA

The kinetic curve of the solution polymerization of TMA is shown in Figure 4. The reaction conditions were as follows: 90°C, 1 : 5 : 10 [Initiator]/[CuBr]/[PMDETA], and PSt-Br-4 as the macroinitiator. The results indicated that the conversion of TMA was 96.4% within 45 h. Therefore, monomer TMA was almost completely consumed within 48 h, and KH570 could be added then to obtain a triblock copolymer instead of a gradient copolymer of the three monomers.

Synthesis of the triblock copolymer and characterization

The results with PSt-Br as the macroinitiator at different reaction times and feed ratios of St, TMA, and KH570 are shown in Table VI. The conversions of the monomers for samples 4#PSTK-2 and 5#PSTK-2, though with longer reaction times than 4#PSTK-1 and 5#PSTK-1 by 16.5 h, only increased slightly more than those of 4#PSTK-1 and 5# PSTK-1, respectively, so the reaction time of 72 h was enough.

As shown in Table VI, the molecular weight distributions were all narrow (within 1.6), indicating a living and controlled reaction. In addition, we noticed that the molecular weights given by GPC were different from the theoretical values. This may be the reason that the poly(3-methacryloxylpropyl trimethoxyl sil-

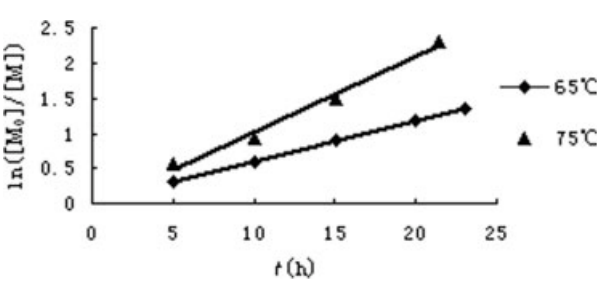

Figure 2 Kinetic curves of the solution polymerization of St in a benzene solution at 65 and 75°C (ATRP).

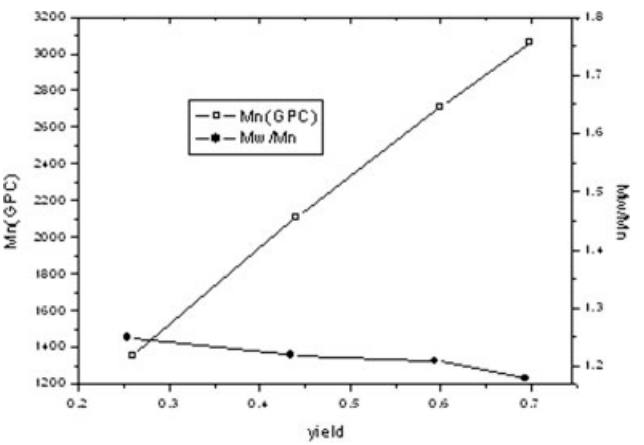

Figure 3 Dependence of M_n and M_w/M_n on the yield in the polymerization of St at 65°C.

TABLE III
Kinetic Parameters and Estimated Concentrations of P· for St Solution ATRP[a]

Temperature (°C)	k_p (L mol^{-1} S^{-1})[b]	k_p^{app} (10^{-5} s^{-1})	[P·] (10^{-7} mol/L)	E_p^{app} (kJ/mol)	A_p^{app}
65	87.51	1.66	1.90		
75	119.50	2.96	2.48	53.04	2644.1
85	160.37	4.75	2.96		

[a] $[St]_0 = 11.65$ mol/L; $[EBriB]_0 = 0.151$ mol/L; [EBriB]/[CuBr]/[PMDETA] = 1 : 1 : 2.
[b] $\ln k_p = 15.32 - 3668.51/T$ (see ref. 27).

ane) (PKH570) block of the triblock copolymer was polar, whereas the standard PS was nonpolar. Therefore, the molecular weights given by GPC may not be very accurate. According to the literature,[30] applying PS calibration curves to GPC analysis of more polarity leads to inaccurate M_w parameters.

The successful synthesis of the PSTK triblock copolymer was confirmed by GPC and the FTIR spectra (Fig. 5). In the FTIR spectra of PSTK, the characteristic peak of the ester group was shown at 1728 cm^{-1}, and the characteristic peak of Si—O—CH_3 was shown at 1032 and 1090 cm^{-1}. The GPC traces of PSt-Br and PSTK had a single peak, and this proved that they were copolymers instead of mixtures of homopolymers. ^{1}H-NMR spectra of the styrene/tetradecyl methyl acrylate diblock copolymer (PST) and triblock PSTK copolymer are shown in Figure 6. Obviously, the ^{1}H-NMR spectrum of PST shows a diagnostic signal centered at 4.0 ppm, characteristic of the methylene in —O—CH_2— of the ester group of TMA. However, besides the characteristics of the methylene in —O—CH_2—, the ^{1}H-NMR spectrum of PSTK shows a diagnostic signal of —O—CH_3 of KH570 centered at 3.6 ppm. At the same time, the intensity of the peaks of the methyl in —O—CH_3 was relatively weak, and this may be ascribed to the low content of KH570 in PSTK.

The molecular weight of PSTK could be calculated via other characteristic peaks from the ^{1}H-NMR spectrum. The polymerization degree of St was calculated by $M_{n,GPC}$ of homopolymer PSt-Br. For diblock PST, on the basis of the intensities of the peaks at 6.5-7.5 ppm ($I_{6.5\text{-}7.5}$) and 3.6-4.1 ppm ($I_{3.6\text{-}4.1}$), the molar ratio of [St]/[TMA] could be calculated according to eq. (5):

$$[St]/[TMA] = (I_{6.5-7.5}/5):(I_{3.6-4.1}/2) \quad (5)$$

Therefore, the ^{1}H-NMR-determined number-average molecular weight ($M_{n,}{}^1$H-NMR) of PSt-Br could be calculated with eq. (6):

$$M_{n,PST} = [TMA] \times M_{TMA} + M_{n,PS} \quad (6)$$

where M_{TMA} is the molecular weight of TMA. For PSTK, on the basis of the intensity of the peaks at 6.5-7.5 ($I_{6.5\text{-}7.5}$) and 3.6-4.1 ppm ($I_{3.6\text{-}4.1}$) for PST and at 6.1-7.5 ($I^*_{6.1-7.5}$) and 3.5-4.2 ppm ($I^*_{3.5-4.2}$) for PSTK, the molar ratio of [St] to [KH570] could be calculated according to eq. (7):

$$[St]/[KH570] = (I^*_{6.1-7.5}/5)/[(I^*_{3.5-4.2} - I^*_{6.1-7.5} \times I_{3.6-4.1}/I_{6.5-7.5})/9] \quad (9)$$

Therefore, $M_{n,}{}^1$H-NMR of PSTK could be calculated with eq. (8), and $M_{n,}{}^1$H-NMR was close to the theoretical number-average molecular weight ($M_{n,theo}$). For example, the molecular weight of sample 4#PSTK-2 calculated according to ^{1}H-NMR was 13,212 g/mol:

$$M_{n,PSTK} = [KH570] \times M_{KH570} + M_{n,PST} \quad (8)$$

where M_{KH570} is the molecular weight of KH570.

TABLE IV
Effects of Different Ligands on the Yield[a]

Sample	Feed ratio ($\times 10^4$ mol)[b]	Time (h)	Temperature (°C)	Yield (%)	$M_{n,GPC}$	$M_{n,theo}$[c]	M_w/M_n
PSt-Br-1	524.4/10.0	6	100	82.0	6790	4680	1.09
PSt-Br-2	524.4/11.0	6	85	81.0	6501	4200	1.20

[a] With bpy as the ligand, [EBriB]/[CuBr]/[bpy] was 1 : 1 : 3; with PMDETA as the ligand, [EBriB]/[CuBr]/[PMDETA] was 1 : 1 : 2.
[b] [St]/[EBriB].
[c] $M_{n,theo}$ = Yield (%) × [Monomer]/[Initiator] × M_n(monomer) + M_n(initiator).

TABLE V
Synthesis and Characterization of the Macroinitiators[a]

Sample	Time (h)	Temperature (°C)	Yield (%)	$M_{n,GPC}$	$M_{n,theo}$[b]	M_w/M_n
PSt-Br-1	18.5	65	58.9	2658	2356	1.20
PSt-Br-2	21.5	65	74.3	3474	2972	1.13
PSt-Br-3	27.0	65	77.2	3215	3088	1.18
PSt-Br-4	21.5	75	89.9	3823	3598	1.10

[a] Volume of St = 4 mL; volume of toluene = 4 mL; [EBriB]/[CuBr]/[PMDETA] = 1 : 1 : 2; [St]/[EBriB] = 0.03496/0.00096 mol/mol.
[b] $M_{n,theo}$ = Yield (%) × [Monomer]/[Initiator] × M_n(monomer) + M_n(initiator).

Contact angle and surface free energy of films coated onto glass plates

According to eq. (9), the dispersion (γ_s^d) and polarity (γ_s^p) of the surface free energy (γ_s) of solids can be calculated by the measurement of the contact angles (θ) of liquids with known surface energy components on a solid film flat surface:

$$(1 + \cos\theta_i)\gamma_i = 4\left(\frac{\gamma_i^d\gamma_s^d}{\gamma_i^d + \gamma_s^d} + \frac{\gamma_i^p\gamma_s^p}{\gamma_i^p + \gamma_s^p}\right) \quad (9)$$

where subscripts i and s represent the liquid and solid film, respectively.

Schultz et al.[31] suggested that the surface free energy of a pure phase (γ) can be expressed by the sum of different intermolecular force components, a London dispersion, and a polar force component, such that

$$\gamma = \gamma^p + \gamma^d \quad (10)$$

where γ^p and γ^d are the dispersion and polar force components, respectively.

The values of γ_i^p and γ_i^d for H_2O and CH_2I_2 are given in Table VII in the literature.[32]

The contact angle of H_2O on a glass plate without treatment was 33.5°, indicating good wetting of H_2O on the glass plate without treatment and a highly polar surface. The contact angle of H_2O on a KH570 film coated onto a glass plate was 76°, whereas that of CH_2I_2 was only 32°. This can be attributed to the chemical reaction between Si—O—CH_3 of KH570 and —OH on the glass plate, leading to a hydrophobic surface and good wetting by CH_2I_2.

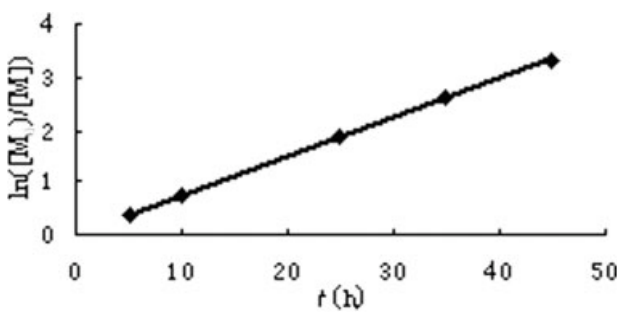

Figure 4 Kinetic curves of the solution polymerization of tetradecyl methyl acrylate at 90°C.

As can be seen in Table VIII, the H_2O contact angles on all the triblock copolymers were higher than those on KH570, whereas CH_2I_2 showed the opposite trend. This could be attributed to the external PTMA block and PS block because the glass reacted with the PKH570 block exclusively. The PTMA block had higher hydrophobicity than KH570 because of its longer side chain, whereas the hydrophobicity of the PS block was similar to that of the PTMA block, so the copolymers possessed better wetting properties than KH570 by CH_2I_2.

In addition, the compositions of the copolymers, illustrated by samples 4#PSTK-1 and 7#PSTK (see Table VI), had little effect on the contact angles of the copolymers with H_2O and CH_2I_2. From the surface energy results, the γ_s^d values of all the copolymers were higher than that of KH570, whereas γ_s^p of all the copolymers was dramatically lower than that of KH570. Moreover, γ_s, γ_s^d, and γ_s^p of copolymer films with different compositions showed only slight differences.

Because both the polypropylene resin and CH_2I_2 were nonpolar, the wetting of the copolymers with a polypropylene melt was similar to that with CH_2I_2. From the good wetting of the copolymers with CH_2I_2, it could be concluded that the copolymers also had good wetting with the polypropylene melt because the copolymers changed the surface structure of the glass fiber and made the surface of the glass fiber more hydrophobic.

The critical concentration of the macromolecular coupling agent was obtained from the curve of the surface free energy versus the concentration. γ_s of 2#PSTK and 4#PSTK-2 solutions decreased linearly as the PSTK mass percentage increased in the range of 0.6%, as shown in Figure 7. However, there was no obvious trend of γ_s when the mass percentages of 2#PSTK and 4#PSTK-2 solution exceeded 0.6 and 0.5%, respectively; this indicated that the copolymer

TABLE VI
Results for PSTKs Prepared via ATRP[a]

Sample	Feed ratio ($\times 10^4$ mol)[b]	Yield (%)	St/TMA/KH570 (wt %) energy spectrum	Time (h)	$M_{n,GPC}$	$M_{n,theo}$[c]	M_w/M_n
1#PSt-Br	1748.08/31.46	88.04		25	5,300	5,282	1.12
1#PSTK	248.2/153.2/17.6	68.50	42/55/3	72.0	15,080	9,482	1.46
2#PSt-Br	2185.1/29.2	89.51		21.5	7,420	7,161	1.15
2#PSTK	113.5/165.3/23.1	50.54	50/46/4	69.5	13,520	8,761	1.33
3#PSt-Br	1748.08/48.05	89.95		20.5	3,710	3,598	1.14
3#PSTK	177.3/241.9/7.1	51.52	40/52/8	69.5	18,561	11,598	1.60
4#PSt-Br	1311.06/76.77	87.06		16.0	1,820	1,741	1.13
4#PSTK-1	230.5/262.1/6.8	52.68	14/84/2	72.0	16,731	11,741	1.54
4#PSTK-2	301.4/221.8/8.9	63.80	24/71/4	88.5	16,997	11,741	1.48
5#PSt-Br	1311.06/59.86	87.69		16.0	2,240	2,192	1.14
5#PSTK-1	212.8/403.2/8.0	40.14	20/78/2	72.0	15,918	10,192	1.59
5#PSTK-2	301.4/403.2/11.1	47.84	12/86/2	88.5	16,102	10,192	1.52
6#PSt-Br	1748.08/34.58	80.5		23	4,580	4,428	1.13
6#PSTK	248.2/76.6/8.8	79.05	33/63/4	72.0	18,176	12,428	1.43
7#PSt-Br	1748.08/23.43	81.28		23	6,612	6,502	1.12
7#PSTK	191.5/80.6/11.8	75.00	53/41/6	72.0	17,900	11,202	1.51

[a] The [Initiator]/[CuBr]/[PMDETA] stoichiometry was 1 : 1 : 2 for samples 1#PSt-Br to 9#PSt-Br, 1 : 5 : 10 for samples 1#PSTK to 3#PSTK, and 1 : 2 : 4 for samples 4#PSTK-1 to 7#PSTK.
[b] For PSt-Br, the feed ratio was [St]/[EBriB]; for PSTK, the feed ratio was [TMA]/[KH570]/[PSt-Br].
[c] For PSt-Br, $M_{n,theo}$(PS) = Yield (%) × [Monomer]/[EBriB] × M_n(monomer) + M_n(EBriB); for PSTK, $M_{n,theo}$ (PSTK) = Yield (%) × σ{[Monomer]/[PSt-Br] × M_n(monomer)} + $M_{n,theo}$(PSt-Br).

solutions reached monolayer saturated adsorption, and the critical concentrations of 2#PSTK and 4#PSTK-2 were 0.6 and 0.5%, respectively. It could be predicted that the glass-fiber-reinforced polypropylene composites would have optimal mechanical properties with that critical concentration because the glass fibers were fully covered. Moreover, if the mass percentage continuously increased, the Si—(OCH_3) quantity of the PSTK film would exceed the Si—OH quantity on the glass fibers, and the PKH570 block of PSTK might be outward to the copolymer film to reduce the wetting of polypropylene on the glass fiber, leading to decreased mechanical properties.

It could be calculated from Figure 7 that the $d\gamma_s/dc$ values of 2#PSTK and 4#PSTK-2 were -28.92×10^{-3} and -22.43×10^{-3} N m^{-1} c^{-1}, respectively. According to the Gibbs adsorptive isotherm [eq. (11)], the monolayer saturated adsorptive capacities of 2#PSTK and 4#PSTK-2 were 7.00×10^{-6} and 4.51×10^{-6} mol/m^2, respectively:

$$\Gamma_2^{(1)} = -\frac{c}{RT}\frac{d\gamma_s}{dc} \tag{11}$$

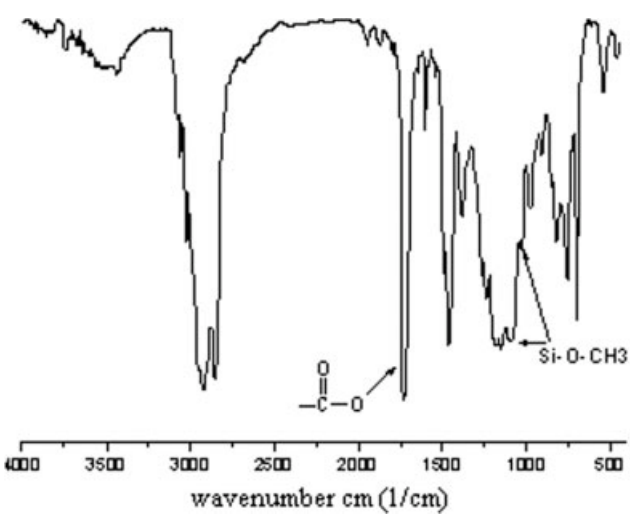

Figure 5 FTIR spectrum of sample 4#PSTK-2.

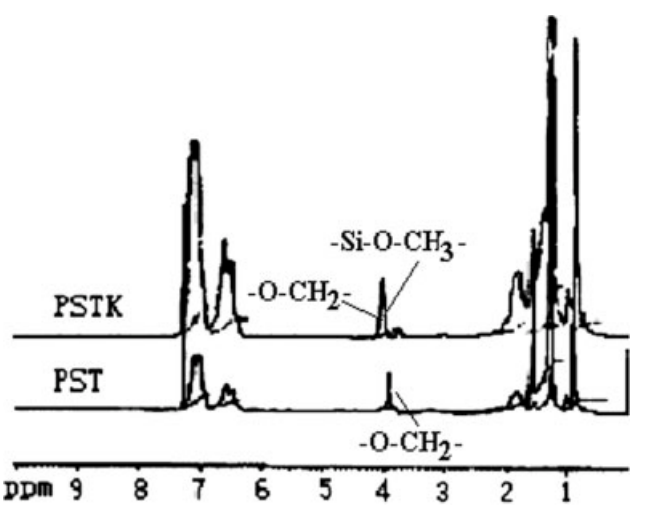

Figure 6 ^{1}H-NMR spectra of PST and 4#PSTK-2.

TABLE VII
Surface Free Energy Characteristics of H_2O and CH_2I_2

	γ_i (mN/m)	γ_i^d (mN/m)	γ_i^p (mN/m)
H_2O	72.8	22.1	50.7
CH_2I_2	50.8	44.1	6.7

where $\Gamma_2^{(1)}$ represents the adsorptive capacity of the copolymer on the surface of glass fiber, c is the mass percentage of the copolymer solution, and γ_s is the surface free energy of the copolymer film.

The areas of 2#PSTK and 4#PSTK-2 could be calculated with the following equations:

$$A = \frac{1}{\Gamma_\infty N_0} = 0.24 \text{ nm}^2$$

$$A' = \frac{1}{\Gamma'_\infty N_0} = 0.37 \text{ nm}^2$$

where N_0 is Avogadro's constant (6.02×10^{23}) and Γ_∞ and Γ'_∞ represent the monolayer saturated adsorption of 2#PSTK and 4#PSTK-2, respectively. A and A′ represent the areas of 2#PSTK and 4#PSTK-2, respectively.

According to the literature,[33] the area of TMA is larger than that of St. The mass percentage of TMA of 4#PSTK-2 should be higher than that of 2#PSTK because of its larger area, and this is consistent with the energy spectrum results for 2#PSTK and 4#PSTK-2 in Table VI.

CONCLUSIONS

A series of triblock copolymers with well-controlled molecular weights and narrow molecular weight distributions were synthesized via ATRP. The results of the kinetic study showed that the optimal reaction conditions were as follows: 1 : 5 : 10 [Initiator]/[CuBr]/[PMDETA], 90°C, and PSt-Br as the macroinitiator. With these copolymers as macromolecular coupling agents coated onto the glass fibers, the wetting by polypropylene on the glass fibers was dramatically improved. The monolayer saturated adsorption on the surface of the glass fibers was indicated by the curves of the surface free energy versus the concentration. The critical concentrations of 2# PSTK and 4#PSTK-2 solutions were 0.6 and 0.5%, respectively, by which it could be predicted that the composites would have the optimal mechanical properties.

TABLE VIII
Contact Angles and Surface Energies of the Films

Sample	Contact angle H_2O	Contact angle CH_2I_2	γ_s (mN/m)	γ_s^d (mN/m)	γ_s^p (mN/m)
KH570	76	32	45.67	34.29	11.38
1#PSTK	92	18	49.86	47.07	2.79
2#PSTK	93	26	47.14	44.38	2.76
3#PSTK	95	18	51.11	49.73	1.38
4#PSTK-1	97	20	54.00	53.50	0.50
4#PSTK-2	93	18	49.80	47.46	2.34
5#PSTK-1	95	19	50.73	49.29	1.44
5#PSTK-2	97	23	52.94	52.46	0.48
6#PSTK	93	17	50.01	47.72	2.29
7#PSTK	92	23	48.47	45.59	2.88

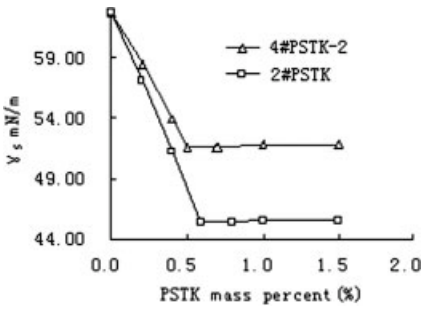

Figure 7 Correlation of γ_s and the PSTK mass percentage.

The authors thank Wu Shusheng for carrying out the surface property analysis.

References

1. Roux, C.; Denault, J.; Michel, F. J Appl Polym Sci 2000, 78, 2047.
2. Xie, H. Q.; Zhang, S.; Xie, D. J Appl Polym Sci 2005, 96, 1414.
3. Arencon, D.; Maspoch, M. L.; Velasco, J. I. Macromol Symp 2003, 200, 225.
4. Yoshiro, N. Asahi Fibreglass Co. Jpn. Pat. WO 2003056095 (2003).
5. Datta, A.; Chen, H. H.; Baird, D. G. Polymer 1993, 34, 759.
6. Wu, T. M.; Lee, C. B. J Appl Polym Sci 1999, 73, 2169.
7. Masaharu, Y.; Masatoshi, O. Prog Org Coat 1996, 27, 277.
8. Zhou, X. D.; Xiong, R. H.; Dai, G. C. Gongneng Gaofenzi Xuebao 2004, 17, 417.
9. Feller, J. F.; Grohens, Y. Compos A 2004, 35, 1.
10. Akira, H.; Toshio, H.; Takahiro, N.; Masao, Y.; Kazuo, Y.; Seiichi, N. Macromolecules 1987, 20, 242.
11. Hideo, S.; Yuka, I.; Tokuzo, K.; Yoshio, H. J Am Chem Soc 1996, 12, 3529.
12. Masashi, K.; Katsuyuki, T.; Yukio, O. Polymer 1995, 36, 535.
13. Qiu, W. L.; Mai, K. C.; Zeng, H. M. J Appl Polym Sci 1999, 71, 1537.
14. Huang, H.; Lu, H. H.; Liu, N. C. J Appl Polym Sci 2000, 78, 1233.
15. Hiroji, F.; Saiko, Y.; Mitsuo, S.; Toshinobu, H. Macromolecules 1996, 29, 1862.
16. Zhao, R. F.; Liu, B.; Dai, G. C.; Hu, C. P. Gaofenzi Cailiao Kexue Yu Gongcheng 2002, 18, 115.
17. Zhang, H. W.; Ai, P.; Jiang, Y.; Li, H. T.; Zhang, K.; Yang, S. R.; Wang, J. Y. Gaodeng Xuexiao Huaxue Xuebao 2004, 25, 2381.
18. Zhang, H. W.; Jiang, Y.; Dong, Y. Q.; Li, H. T.; Zhang, K.; Wang, J. Y. Polym Mater Sci Eng 2004, 90, 401.

19. Xu, F. J.; Cai, Q. J.; Kang, E. T.; Neoh, K. G. Macromolecules 2005, 38, 1051.
20. Nguyen, J. V.; Jones, C.; Design, W. Macromolecules 2004, 37, 1190.
21. Granville, A. M.; Boyes, S. G.; Akgun, B.; Foster, M. D.; Brittain, W. J. Macromolecules 2004, 37, 2790.
22. Hamelinck, P. J.; Huck Wilhelm, T. S. J Mater Chem 2005, 15, 381.
23. Lee, S. B.; Koepsel, R. R.; Morley, S. W.; Matyjaszewski, K.; Sun, Y.; Russell, A. J. Biomacromolecules 2004, 5, 877.
24. Keller, R. N.; Wycoff, H. D. Inorg Synth 1946, 2, 1.
25. Carroll, B. J. J Colloid Interface Sci 1976, 57, 488.
26. Yamaki, J.; Katayama, Y. J Appl Polym Sci 1975, 19, 2897.
27. Pan, Z. R. Polymer Chemistry, 1st ed.; Chemical Industry: Beijing, 1986.
28. Matyjaszewski, K.; Patten, T. E.; Xia, J. J Am Chem Soc 1997, 119, 674.
29. Goto, A.; Fukuda, T. Prog Polym Sci 2004, 29, 329.
30. Dubin, P.; Koontz, S. J Polym Sci Polym Chem Ed 1977, 15, 2047.
31. Schultz, J.; Tsutsumi, K.; Razouk, B. J. J Colloid Interface Sci 1977, 59, 277.
32. Gao, P.; Su, K. B.; Ward, Y.; Weng, L. T. Polym Compos 2000, 21, 312.
33. Wu, S. H. Polymer Interface and Adhesion; Marcel Dekker: New York, 1982.